Proceeding of the IEEE
International Conference on Robotics and Biomimetics
Dali, China, December 2019

Sigmoid Super-Twisting Extended State Observer and Sliding Mode Controller for Quadrotor UAV Attitude System With Unknown Disturbance

Yongfeng Rong, Ran Jiao and Song Kang
College of Mechanical Engineering and Automation
Beihang University
Beijing, China
{ryf_2018, jiaoran, kangsong}@buaa.edu.cn

Wusheng Chou
The State Key Laboratory of Virtual Reality
Technology and Systems
Beihang University
Beijing, China
wschou@buaa.edu.cn

***Abstract*— The super-twisting algorithm has been verified its effectiveness in attitude control for quadrotor with unknown disturbance. However, the discontinuous signum function in super-twisting formulation causes the unwanted chattering problem and thus affects the attitude control performance. In this paper, we replace the signum function with sigmoid function and propose the sigmoid super-twisting extended state observer (SSTESO) and sliding mode controller (SSTSMC). Besides, a rigorous convergence analysis of proposed nonlinear error system based on the Lyapunov stability theory is performed, and the parameter selection rule is given. Numerical simulations are implemented in presence of manually designed disturbance in order to verify the advantage of the proposed algorithm compared with original super-twisting algorithm. Results show that the introduction of sigmoid function can not only reduce the chattering effect, but also maintain the advantage of super-twisting algorithm.**

***Index Terms*— Quadrotor attitude control; active disturbance rejection control (ADRC); sigmoid super twisting extended state observer (SSTESO); sigmoid super twisting sliding mode controller (SSTSMC)**

I. Introduction

In recent years, unmanned aerial vehicles (UAVs) have attracted more and more attention due to their small size, low cost and easy maintainability [1]. Quadrotor is a kind of UAV that has four propellers driven by four direct current (DC) motors respectively [2]. It has a wide range of applications including supervision, pesticide spraying, aerial photography, environmental monitoring, mapping and even transportation [3]–[5]. Due to its underactuation and high non-linearity, the control of the quadrotor is a challenging problem [6].

Among all the control problems, the attitude control is the primary and basic problem, and a number of control methods have been researched [7]. In practical engineering, the classical controller such as PID controller [8] is usually used. However, PID controller is not robust to unknown external disturbance [9]. Thus, the modern control theory is introduced, such as backstepping control [10], robust and adaptive control [11] and so on. In the real fight environments, quadrotor may suffer from disturbance and uncertainties such as wind gust, parametric uncertainties and actuator faults, which may lead to stability problem. Sliding mode control (SMC) for quadrotor [12] is proposed to suppress the effects of disturbance and stabilize the control system, but the chattering problem induced by the discontinuous signum function limits its applications.

The aforementioned methods are all passive antidisturbance control (PADC) methods, which can not react fast enough when dealing with strong disturbance. The active antidisturbance control (AADC), including disturbance observer based control (DOBC) and active disturbance rejection control (ADRC) [13], are then proposed to improve the ability to resist external disturbance [14]. The key part of ADRC is to estimate the disturbance using an extended state observer (ESO), which merges the disturbance and system states into an augmented state vector and gives compensation to the controller to resist the disturbance. However, traditional ESO can not estimate the sudden disturbance thoroughly such as wind gust and actuator faults. Thus, amounts of modified ESO have been proposed and used in quadrotor attitude control, such as an improved ESO in [15], a high-order ESO in [16] and super-twisting ESO (STESO) in [17]. In particular, the STESO can not only estimate the sudden disturbance accurately in a finite time, but also avoid excessively high observer gain. However, there is also a discontinuous signum function in its estimation law which causes chattering problem in estimation [18].

To reduce the chattering problem in the controller or observer, some previous work has been done. A common way to reduce chattering in SMC is to introduce a boundary layer, which is usually an approximate piecewise function [19]. In [20], a multivariable supertwisting-like algorithm (STLA) is proposed to reduce chattering based on STSMC. However, these methods are all focused on controllers. The chattering

Corresponding author: Ran Jiao Email: jiaoran@buaa.edu.cn

978-1-7281-6321-5/19//$31.00 ©2019 IEEE

problem also exists in super-twisting observers. The most similar work with us is [21], in which a sigmoid function based novel tracking differentiator (STD) is used, but they do not combine it with the super-twisting method.

The main contributions of this paper are summarized as follows.

- By replacing the discontinuous signum function with fully continuous sigmoid function, a sigmoid super-twisting extended state observer (SSTESO) and a sigmoid super-twisting sliding mode controller (SSTSMC) are proposed to reduce the chattering problem and meanwhile maintain the advantages of super-twisting algorithm.
- A comprehensive stability analysis of the entire system with a nonlinear sigmoid term and the parameter selection rule are given base on SSTESO and SSTSMC. Simulation experiments are presented to verify the advantages of proposed algorithm.

II. Preliminaries

A. Notation

The bold symbols are used to define vectors or matrix. The vectors defined in this paper are assumed to be column vectors without loss of generality. $\|\bullet\|$ denotes the 2-norm of a vector, which can be calculated by $\|\boldsymbol{v}\| = \sqrt{\boldsymbol{v}^T\boldsymbol{v}}$ for a specific vector $\boldsymbol{v}$. Moreover, the skew symmetric matrix of $\boldsymbol{v} = \begin{bmatrix} v_1 & v_2 & v_3 \end{bmatrix}^T$ is given as

$$\boldsymbol{S}(\boldsymbol{v}) = \begin{bmatrix} 0 & -v_1 & v_2 \\ v_1 & 0 & -v_3 \\ -v_2 & v_3 & 0 \end{bmatrix} \quad (1)$$

B. Quaternion Operation

A unit quaternion is an appropriate choice for representing rotation of the quadrotor, which can avoid the singularity problem of trigonometric functions. Define $\boldsymbol{q} = \begin{bmatrix} q_0 & \boldsymbol{q}_v^T \end{bmatrix}^T \in \mathbb{R}^4$, $\|\boldsymbol{q}\| = 1$ and then we have the following operation.

The derivative of quaternion is

$$\dot{\boldsymbol{q}} = \begin{bmatrix} \dot{q}_0 \\ \dot{\boldsymbol{q}}_v \end{bmatrix} = \frac{1}{2}\boldsymbol{q} \otimes \begin{bmatrix} 0 \\ \boldsymbol{\omega} \end{bmatrix} = \frac{1}{2}\begin{bmatrix} -\boldsymbol{q}_v^T \\ \boldsymbol{S}(\boldsymbol{q}_v) + q_0\boldsymbol{I}_3 \end{bmatrix}\boldsymbol{\omega} \quad (2)$$

where $\boldsymbol{\omega}$ is the angular velocity of the system.

The quaternion error $\boldsymbol{q}_e$ between the actual quaternion $\boldsymbol{q}$ and the desired quaternion $\boldsymbol{q}_d$ is given as

$$\boldsymbol{q}_e = \boldsymbol{q}_d \otimes \boldsymbol{q} = \begin{bmatrix} q_0 q_{0d} - \boldsymbol{q}_v^T\boldsymbol{q}_{vd} \\ q_{0d}\boldsymbol{q}_v + q_0\boldsymbol{q}_{vd} - \boldsymbol{S}(\boldsymbol{q}_v)\boldsymbol{q}_{vd} \end{bmatrix} \quad (3)$$

The transform between rotation matrix $\boldsymbol{R}_A^B$ and corresponding quaternion $\boldsymbol{q}$ is

$$\boldsymbol{R}_A^B = (q_0^2 - \boldsymbol{q}_v^T\boldsymbol{q}_v)\boldsymbol{I}_3 + 2\boldsymbol{q}_v\boldsymbol{q}_v^T + 2q_0\boldsymbol{S}(\boldsymbol{q}_v) \quad (4)$$

and its derivate is

$$\dot{\boldsymbol{R}}_A^B = -\boldsymbol{S}(\boldsymbol{\omega})\boldsymbol{R}_A^B \quad (5)$$

C. Kinematics and Dynamics of Quadrotor

In this section, the kinematics and dynamics of the quadrotor are introduced. To simplify the modeling of quadrotor, four reasonable assumptions are made:

Assumption 1. Quadrotor is symmetric with respect to both x-axis and y-axis.

Assumption 2. Quadrotor works in low motion speed so that the aerodynamic effects can be omitted.

Assumption 3. The rotors have no blade flapping effect.

Assumption 4. Quadrotor is subjected to bounded unknown external disturbance.

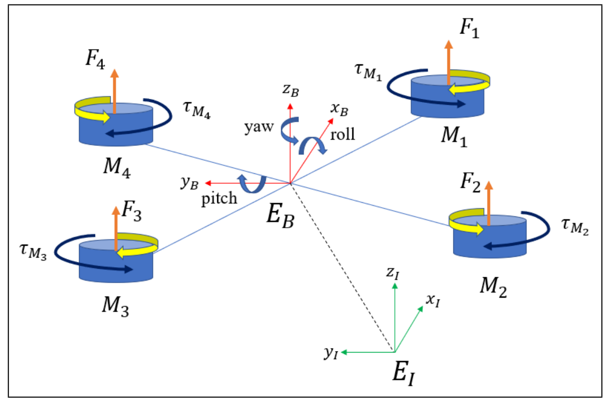

Fig. 1. Quadrotor model and its coordinate system

The simplified model is shown in Fig. 1. As described in [22], the rotation of four rotors $M_i(i = 1, ..., 4)$ generates thrusts $F_i = k_T\Omega_i^2(i = 1, ..., 4)$, where Ω_i is the angular speed of rotor M_i and k_T denotes the thrust factor. The reaction torque $\tau_{M_i} = k_D\Omega_i^2$, where k_D is the drag factor. The total relationship between angular speed and input torque is given as follows:

$$\begin{bmatrix} \tau_\phi \\ \tau_\theta \\ \tau_\psi \end{bmatrix} = \begin{bmatrix} -\frac{l}{\sqrt{2}}k_T & -\frac{l}{\sqrt{2}}k_T & \frac{l}{\sqrt{2}}k_T & \frac{l}{\sqrt{2}}k_T \\ -\frac{l}{\sqrt{2}}k_T & \frac{l}{\sqrt{2}}k_T & \frac{l}{\sqrt{2}}k_T & -\frac{l}{\sqrt{2}}k_T \\ k_D & -k_D & k_D & -k_D \end{bmatrix}\begin{bmatrix} \Omega_1^2 \\ \Omega_2^2 \\ \Omega_3^2 \\ \Omega_4^2 \end{bmatrix} \quad (6)$$

where $\boldsymbol{\tau} = \begin{bmatrix} \tau_\phi & \tau_\theta & \tau_\psi \end{bmatrix}^T$ denotes the torque applied to roll, pitch and yaw, respectively and l represents the distance between two rotors with the same rotation direction.

In addition, two coordinate frames are introduced in Fig. 1, including the body frame $E_B : \{x_B, y_B, z_B\}$ and the inertial frame $E_I : \{x_I, y_I, z_I\}$. The attitude of the quadrotor relative to inertial frame is described by a unit quaternion $\boldsymbol{q} = \begin{bmatrix} q_0 & \boldsymbol{q}_v^T \end{bmatrix}^T$, $\|\boldsymbol{q}\| = 1$. The angular velocities relative to body frame along three axes are defined as $\boldsymbol{\omega} = \begin{bmatrix} \omega_x & \omega_y & \omega_z \end{bmatrix}^T$. The kinematic transform between $\dot{\boldsymbol{q}}$ and $\boldsymbol{\omega}$ is given in (2).

Based on Newton-Euler theory, the dynamic model of quadrotor can be obtained as:

$$\dot{\boldsymbol{\omega}} = -\boldsymbol{J}^{-1}\boldsymbol{S}(\boldsymbol{\omega})\boldsymbol{J}\boldsymbol{\omega} + \boldsymbol{J}^{-1}\boldsymbol{u} + \boldsymbol{J}^{-1}\boldsymbol{d} \quad (7)$$

where $\boldsymbol{J}=diag(J_x,J_y,J_z)$ is a diagonal matrix denoting the nominal inertia of the quadrotor and $\boldsymbol{d}=\begin{bmatrix} d_x & d_y & d_z \end{bmatrix}^T$ denotes the lumped disturbance reacted on the quadrotor. $\boldsymbol{u}=\begin{bmatrix} u_x & u_y & u_z \end{bmatrix}^T=\boldsymbol{\tau}$ is the control law to be designed.

D. Problem Formulation

The error vector of angular velocities relative to body frame is given as

$$\boldsymbol{\omega}_e=\boldsymbol{\omega}-\boldsymbol{R}_A^B\boldsymbol{\omega}_d \tag{8}$$

where $\boldsymbol{\omega}_d$ is the desired angular velocities given in inertia frame and $\boldsymbol{\omega}$ is the current velocities measured by sensors with respect to body frame. $\boldsymbol{R}_A^B$ is the rotation matrix between the two frames and can be calculated base on (4).

The derivative of $\boldsymbol{\omega}_e$ can be derived according to (5), (7) and (8).

$$\dot{\boldsymbol{\omega}}_e=\boldsymbol{S}(\boldsymbol{\omega}_d)\boldsymbol{R}_A^B\boldsymbol{\omega}_d-\boldsymbol{R}_A^B\dot{\boldsymbol{\omega}}_d-\boldsymbol{J}^{-1}\boldsymbol{S}(\boldsymbol{\omega})\boldsymbol{J}\boldsymbol{\omega}+\boldsymbol{J}^{-1}\boldsymbol{u}+\boldsymbol{J}^{-1}\boldsymbol{d} \tag{9}$$

The attitude tracking error $\dot{\boldsymbol{q}}_e$ relative to desired attitude $\dot{\boldsymbol{q}}_d$ can be obtained by (2), (3) and (8).

$$\dot{\boldsymbol{q}}_e=\begin{bmatrix} \dot{q}_{0e} \\ \dot{\boldsymbol{q}}_{ve} \end{bmatrix}=\frac{1}{2}\boldsymbol{q}_e\otimes\begin{bmatrix} 0 \\ \boldsymbol{\omega}_e \end{bmatrix}=\frac{1}{2}\begin{bmatrix} -\boldsymbol{q}_{ve}^T \\ \boldsymbol{S}(\boldsymbol{q}_{ve})+q_{0e}\boldsymbol{I}_3 \end{bmatrix}\boldsymbol{\omega}_e \tag{10}$$

The goal of designing observer and controller for quadrotor is to obtain high precision tracking performance in the presence of unknown lumped disturbance $\boldsymbol{d}$. The errors of the attitude angles $\boldsymbol{q}_e$ and the angular velocities $\boldsymbol{\omega}_e$ should be guaranteed to converge to a bounded ball under the designed control law $\boldsymbol{u}$.

III. Design and Analysis of Sigmoid Super Twisting Extended State Observer

The lumped disturbances acting on the quadrotor are usually high-order and rapidly changing. In the work of [17], the super-twisting extended state observer (STESO) is proposed to estimate the disturbance. Although STESO can avoid higher control gains compared with traditional ESO, it has signum functions in the estimation law that may cause discontinuous disturbance estimation, which leads to unwanted chattering in the performance and thus affects the controller performance. By replacing the discontinuous signum function with continuous function, the chattering effect can be reduced. In this section, the sigmoid super twisting extender state observer (SSTESO) is proposed first, and then convergence analysis and parameter selection rule are presented.

A. Design of SSTESO

Using the same feedback linearization technique in [17], the control input can be reformulated as

$$\boldsymbol{u}^*=\boldsymbol{u}-\boldsymbol{S}(\boldsymbol{\omega})\boldsymbol{J}\boldsymbol{\omega} \tag{11}$$

Then the model of quadrotor can be linearized as

$$\boldsymbol{J}\dot{\boldsymbol{\omega}}=\boldsymbol{u}^*+\boldsymbol{d} \tag{12}$$

We assume that each component of the linearized model is independent. Therefore, the estimation law derived from one channel can be applied to the others. The one-channel model can be derived as

$$J_i\dot{\omega}_i={u_i}^*+d_i \tag{13}$$

where $i=x,y,z$ denotes the i-th channel.

According to Assumption 4, the lumped disturbance d should be a Lipschitz continuous signal. The time derivative of the lumped disturbance terms d_i thus exists almost everywhere, and it is bounded, formulated by

$$\left|\dot{d}_i\right|\le\gamma^+ \tag{14}$$

By defining a new state vector $\boldsymbol{X}_i=\begin{bmatrix} x_{1,i} & x_{2,i} \end{bmatrix}^T$, where $x_{1,i}=J_i\omega_i$ and $x_{2,i}=d_i$, the extended state equation of (13) can be written as

$$\begin{cases} \dot{x}_{1,i}=x_{2,i}+{\tau_i}^* \\ \dot{x}_{2,i}=\varepsilon_i \end{cases} \tag{15}$$

where ε_i denotes the derivative of d_i.

Based on the above system, the following SSTESO is designed to estimate the lumped disturbance.

$$\begin{cases} \dot{\hat{x}}_{1,i}=\hat{x}_{2,i}+{\tau_i}^*+\lambda_{1,i}|x_{1,i}-\hat{x}_{1,i}|^{\frac{1}{2}}\operatorname{sgn}(x_{1,i}-\hat{x}_{1,i}) \\ \dot{\hat{x}}_{2,i}=\lambda_{2,i}sig(x_{1,i}-\hat{x}_{1,i}) \end{cases} \tag{16}$$

with

$$sig(\xi)=\frac{1-e^{-\beta\xi}}{1+e^{-\beta\xi}} \tag{17}$$

and

$$\operatorname{sgn}(a)=\begin{cases} \frac{a}{|a|}, & a\neq 0 \\ 0, & a=0 \end{cases} \tag{18}$$

where $\lambda_{1,i}$, $\lambda_{2,i}$ and β are the observer gains to be designed.

As can be seen from (16), the signum function is substituted by the continuous function $sig(\xi)$. The chosen function is limited by $[-1,1]$, the same as signum function. One of the advantages of the chosen function is that by adjusting the parameter β, we can find a balance between nonchattering effect and good tracking performance.

Define the estimation error vector $\tilde{\boldsymbol{X}}_i=\begin{bmatrix} \tilde{x}_{1,i} & \tilde{x}_{2,i} \end{bmatrix}^T$ where $\tilde{x}_i=x_i-\hat{x}_i$. According to the above definition, the error system is described as

$$\begin{cases} \dot{\tilde{x}}_{1,i}=\tilde{x}_{2,i}-\lambda_{1,i}|\tilde{x}_{1,i}|^{\frac{1}{2}}\operatorname{sgn}(\tilde{x}_{1,i}) \\ \dot{\tilde{x}}_{2,i}=-\lambda_{2,i}sig(\tilde{x}_{1,i})+\varepsilon_i \end{cases} \tag{19}$$

The convergence of the error system is not obvious, but through our following analysis, the errors $\tilde{x}_{1,i}$ and $\tilde{x}_{1,i}$ will be guaranteed to converge to a small bounded ball as time goes to infinity if observer gains $\lambda_{1,i}$, $\lambda_{2,i}$ and β are selected properly. Besides, a parameter selection rule is given to satisfy the convergence conditions after the analysis.

B. Convergence Analysis and Parameter Selection Rule

Without loss of generality, we rewrite the formulation and omit the i subscript in the following analysis for simplified representation.

$$\left\{\begin{array}{l}\dot{z}_1 = z_2 - \lambda_1 |z_1|^{\frac{1}{2}} \mathrm{sgn}(z_1) \\ \dot{z}_2 = -\lambda_2 sig(z_1) + \varepsilon\end{array}\right. \tag{20}$$

where $z_1 = \tilde{x}_1$ and $z_2 = \tilde{x}_2$ with i subscript omitted.

Introduce a new state vector $\boldsymbol{\mu} = [\begin{array}{cc}\mu_1 & \mu_2\end{array}]$ where $\mu_1 = |z_1|^{\frac{1}{2}} sgn(z_1)$ and $\mu_2 = z_2$.

Take the time derivative of $\boldsymbol{\mu}$ and we get

$$\left\{\begin{array}{l}\dot{\mu}_1 = \frac{1}{2}|z_1|^{-\frac{1}{2}}(-\lambda_1\mu_1 + \mu_2) \\ \dot{\mu}_2 = -\lambda_2 sig(z_1) + \varepsilon\end{array}\right. \tag{21}$$

The Lyapunov function V can be chosen as

$$V = \boldsymbol{\mu}^T \boldsymbol{P} \boldsymbol{\mu} \tag{22}$$

where

$$\boldsymbol{P} = \frac{1}{2}\left[\begin{array}{cc}\lambda_1^2 + 4\lambda_2 & -\lambda_1 \\ -\lambda_1 & 2\end{array}\right] \tag{23}$$

is a positive definite matrix when $\lambda_1 > 0$ and $\lambda_2 > 0$.

The time derivative of V is derived in details in the Appendix part, and the result is

$$\begin{aligned}\dot{V} \leq & -\frac{\lambda_1}{2}|z_1|^{-\frac{1}{2}}[(\lambda_1^2 + 2\lambda_2 - \frac{2\lambda_2}{\lambda_1\sqrt{\beta}})|\mu_1|^2 - 2\lambda_1|\mu_1||\mu_2| \\ & + (1 - \frac{2\lambda_2}{\lambda_1\sqrt{\beta}})|\mu_2|^2] + \frac{\lambda_1}{2}|z_1|^{-\frac{1}{2}}(2|\mu_1|^2 + \frac{2}{\lambda_1}|\mu_1|^2 \\ & + \frac{2}{\lambda_1}|\mu_2|^2)\gamma^+\end{aligned} \tag{24}$$

Define

$$\boldsymbol{\Gamma} = \left[\begin{array}{cc}\lambda_1^2 + 2\lambda_2 - \frac{2(\lambda_1+1)\gamma^+}{\lambda_1} & -\lambda_1 \\ -\lambda_1 & 1 - \frac{2\gamma^+}{\lambda_1} - \frac{4\lambda_2}{\lambda_1\sqrt{\beta}}\end{array}\right] \tag{25}$$

Then, Equation (24) can be rewritten as

$$\begin{aligned}\dot{V} & \leq -\frac{\lambda_1}{2}|z_1|^{-\frac{1}{2}}(\boldsymbol{\mu}^T\boldsymbol{\Gamma}\boldsymbol{\mu} - \frac{\lambda_2}{\lambda_1\sqrt{\beta}}) \\ & \leq -\frac{\lambda_1}{2}|z_1|^{-\frac{1}{2}}(\sigma_{\min}(\boldsymbol{\Gamma})\|\boldsymbol{\mu}\|^2 - \frac{\lambda_2}{\lambda_1\sqrt{\beta}})\end{aligned} \tag{26}$$

where $\sigma_{\min}(\boldsymbol{\Gamma})$ is the minimum eigenvalue of the positive definite matrix $\boldsymbol{\Gamma}$. It can be concluded that $\dot{V} < 0$ whenever $\|\boldsymbol{\mu}\|^2 \geq \frac{\lambda_2}{\sigma_{\min}(\boldsymbol{\Gamma})\lambda_1\sqrt{\beta}}$. Thus, the upper bound of estimation error $\|\boldsymbol{\mu}\|^2$ will be constrained by the bounded ball $\boldsymbol{B}_{\boldsymbol{\mu}} = \{\boldsymbol{\mu} | \|\boldsymbol{\mu}\|^2 \leq \frac{\lambda_2}{\sigma_{\min}(\boldsymbol{\Gamma})\lambda_1\sqrt{\beta}}\}$. It is worth pointing out that when $\beta \to \infty$, the convergence conditions will be the same as STESO [17], which is consistent with our intuition.

By choosing appropriate observer gains $\lambda_1 > 0$, $\lambda_2 > 0$ and $\beta > 0$, $\boldsymbol{\Gamma}$ can be a positive definite matrix. The parameter selection rule is given as follows.

$$\left\{\begin{array}{l}\lambda_1 - 2\gamma^+ + \frac{4\lambda_2}{\sqrt{\beta}} > 0 \\ (\frac{2\gamma^+}{\lambda_1} + \frac{4\lambda_2}{\lambda_1\sqrt{\beta}} - 1)(\lambda_2 + 2\gamma^+ + \frac{2\gamma^+}{\lambda_1} - \lambda_1^2) - \lambda_1^2 > 0\end{array}\right. \tag{27}$$

To further explain how the observer gain β affects the convergence rate of the system, we adopt the method used in [21]. The Taylor expansion of the sigmoid function at the origin is

$$sig(x) = \frac{\beta x}{2} - \frac{(\beta x)^3}{24} + \frac{(\beta x)^5}{240}\dots \tag{28}$$

We discuss the effect of sigmoid function in the following two cases.

Case 1. When $|\beta x| < 1$, the linear term of the sigmoid function domains the performance of the system. Thus, the system will exponentially converge to the equilibrium point. Most importantly, the undesired chattering problem is reduced because of the linear term. In that case, (21) can be rewritten as

$$\left\{\begin{array}{l}\dot{\mu}_1 = \frac{1}{2}|z_1|^{-\frac{1}{2}}(-\lambda_1\mu_1 + \mu_2) \\ \dot{\mu}_2 = -\lambda_2\frac{\beta z_1}{2} + \varepsilon\end{array}\right. \tag{29}$$

Case 2. When $|\beta x| \geq 1$, the nonlinear term of sigmoid function plays a dominant role in the performance of the system. When β is chosen large enough, the sigmoid function will perform approximately to the signum function. The system can perform the same characteristic as STESO.

IV. Design of Sigmoid Super Twisting Sliding Mode Controller

SMC has been verified its availability by many researchers for its advantages in systems suffering from disturbances and uncertainties. However, chattering problem always exists in SMC methods, including traditional SMC and super-twisting sliding mode control (STSMC). In order to reduce the chattering effect and still keep the advantages of STSMC, we replace the signum function with the proposed continuous function and introduce a sigmoid super-twisting sliding mode controller (SSTSMC). The sliding mode manifold is chosen as

$$\boldsymbol{s} = \boldsymbol{\alpha}_1\boldsymbol{q}_{ev} + \boldsymbol{J}\boldsymbol{\omega}_e \tag{30}$$

where $\boldsymbol{\alpha}_1 = diag(\alpha_{1,\phi}, \alpha_{1,\theta}, \alpha_{1,\psi})$ is a positive definite diagonal matrix to be designed.

The time derivation of $\boldsymbol{s} = [\begin{array}{ccc}s_\phi & s_\theta & s_\psi\end{array}]^T$ is

$$\dot{\boldsymbol{s}} = \boldsymbol{\alpha}_1\dot{\boldsymbol{q}}_{ev} + \boldsymbol{J}\dot{\boldsymbol{\omega}}_e \tag{31}$$

Substitute (9) into (31), we get

$$\dot{\boldsymbol{s}} = \boldsymbol{\alpha}_1\dot{\boldsymbol{q}}_{ev} + \boldsymbol{u} + \boldsymbol{d} + \boldsymbol{J}(\boldsymbol{S}(\boldsymbol{\omega}_d)\boldsymbol{R}_a^b\boldsymbol{\omega}_d - \boldsymbol{R}_a^b\dot{\boldsymbol{\omega}}_d) - \boldsymbol{S}(\boldsymbol{\omega})\boldsymbol{J}\boldsymbol{\omega} \tag{32}$$

Then, the SSTSMC control law is designed as

$$\begin{aligned}\boldsymbol{u} = &-(\boldsymbol{J}(\boldsymbol{S}(\boldsymbol{\omega}_d)\boldsymbol{R}_a^b\boldsymbol{\omega}_d - \boldsymbol{R}_a^b\dot{\boldsymbol{\omega}}_d) - \boldsymbol{S}(\boldsymbol{\omega})\boldsymbol{J}\boldsymbol{\omega}) - \boldsymbol{\alpha}_1\dot{\boldsymbol{q}}_{ev} \\ &- \boldsymbol{\alpha}_2|\boldsymbol{s}|^{\frac{1}{2}}\operatorname{sgn}(\boldsymbol{s}) - \int_0^t \boldsymbol{\alpha}_3 sig(\boldsymbol{s})d\tau - \hat{\boldsymbol{d}}\end{aligned} \tag{33}$$

where $sig(\boldsymbol{s})$ is defined in (17). By combining (32) and (33), we get

$$\dot{\boldsymbol{s}} = -\boldsymbol{\alpha}_2|\boldsymbol{s}|^{\frac{1}{2}}\operatorname{sgn}(\boldsymbol{s}) - \int_0^t \boldsymbol{\alpha}_3 sig(\boldsymbol{s})d\tau + \tilde{\boldsymbol{d}} \tag{34}$$

where $\tilde{\boldsymbol{d}} = \boldsymbol{d} - \hat{\boldsymbol{d}}$ is the estimation error of lumped disturbance $\boldsymbol{d}$. The positive definite diagonal matrix $\boldsymbol{\alpha}_2 = diag(\alpha_{2,\phi}, \alpha_{2,\theta}, \alpha_{2,\psi})$, $\boldsymbol{\alpha}_3 = diag(\alpha_{3,\phi}, \alpha_{3,\theta}, \alpha_{3,\psi})$ and $\boldsymbol{\beta} = diag(\beta_\phi, \beta_\theta, \beta_\psi)$ in sigmoid function $sig(\boldsymbol{s})$ are the controller gains to be designed. The convergence of the propose law is guaranteed by using the same analysis method as previous section. Define $\boldsymbol{\zeta} = -\int_0^t \boldsymbol{\alpha}_3 sig(\boldsymbol{s})d\tau + \tilde{\boldsymbol{d}}$ and rewrite (34) as

$$\begin{cases} \dot{\boldsymbol{s}} = \dot{\boldsymbol{\zeta}} - \boldsymbol{\alpha}_2|\boldsymbol{s}|^{\frac{1}{2}}\operatorname{sgn}(\boldsymbol{s}) \\ \dot{\boldsymbol{\zeta}} = -\boldsymbol{\alpha}_3 sig(\boldsymbol{s})d\tau + \dot{\tilde{\boldsymbol{d}}} \end{cases} \tag{35}$$

It can be also verified that the system error of (35) is limited by a bounded ball. The process of convergence analysis can be referred to the previous section. The resultant parameter selection rule is given as follows.

$$\begin{cases} \alpha_{2,i} - 2\left\|\dot{\tilde{d}}_i\right\| + \frac{4\alpha_{3,i}}{\sqrt{\beta_i}} > 0 \\ (\frac{2\left\|\dot{\tilde{d}}_i\right\|}{\alpha_{2,i}} + \frac{4\alpha_{3,i}}{\alpha_{2,i}\sqrt{\beta_i}} - 1)(\alpha_{3,i} + 2\left\|\dot{\tilde{d}}_i\right\| + \frac{2\left\|\dot{\tilde{d}}_i\right\|}{\alpha_{2,i}} - \alpha_{2,i}^2) - \alpha_{2,i}^2 > 0 \end{cases} \tag{36}$$

where $i = \phi, \theta, \psi$.

V. Simulation Result and Analysis

To validate the effectiveness and superiority of the proposed improvement based on super-twisting algorithm, two numerical simulations are presented in this section. The simulations are done in PX4/Gazebo [23] environment.

A. Simulation I: SSTESO vs. STESO

To verify the advantages of introducing a sigmoid function into STESO, we compare the estimation performance of the two observers using manual inserted disturbance with the quadrotor hovering. In order to compare the observers only, we both use default PID controller in open-source PIXHAWK [24]. The manually designed disturbance is applied on both roll and pitch channels, and its formulation is given as follows:

$$d = 0.01\sin(0.5t + 1) + 0.02\sin(0.1t + 3) + 0.04\sin(t + 0.5) \tag{37}$$

The observer gains set in the simulation is given in TABLE I.

TABLE I

Quadrotor parameters used in simulation I

Observer	Parameters
STESO	$\boldsymbol{\lambda}_1 = 0.2\boldsymbol{I}, \boldsymbol{\lambda}_2 = 0.01\boldsymbol{I}$
SSTESO	$\boldsymbol{\lambda}_1 = 0.4\boldsymbol{I}, \boldsymbol{\lambda}_2 = 0.2\boldsymbol{I}, \boldsymbol{\beta} = 100\boldsymbol{I}$

Fig. 2 shows the disturbance estimation results on the roll, pitch and yaw channels of SSTESO and STESO with the parameters setting and manual disturbance mentioned in (37) and TABLE I. In addition, the root-mean-square (RMS) estimation errors are shown in TABLE II. It can be seen that both observers can have good performance in tracking the disturbance. However, it is obvious that SSTESO has less chattering effect all in three channels compared with STESO, which verifies the power of introducing the sigmoid function into STESO and provides strong proof to the theoretical analysis.

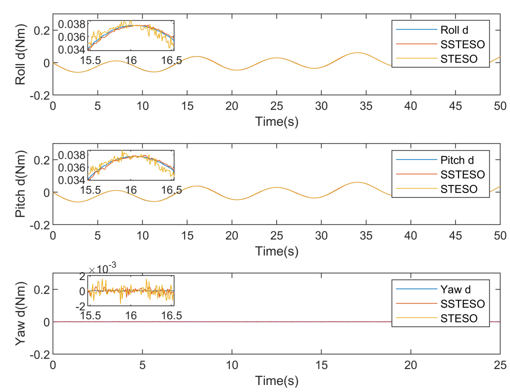

Fig. 2. Disturbance estimation results in Simulation I

TABLE II

Comparison of disturbance estimation performance: RMS error($Nm \times 10^{-4}$)

	Roll	Pitch	Yaw
STESO	3.8597	3.8518	2.6942
SSTESO	4.3326	4.9020	6.7907

B. Simulation II: Proposed Method vs. Traditional Super Twisting Method

In order to compare the attitude control performance of quadrotor subjected to lumped disturbance using both controllers and observers, we present a simulation between STESO+STSMC and SSTESO+SSTSMC with the hovering mission for quadrotor. The disturbance used in this simulation is the same as (37). The system parameters are shown in

TABLE III.

TABLE III

QUADROTOR PARAMETERS USED IN SIMULATION II

Observer/Controller	Parameters
STESO	$\boldsymbol{\lambda}_1 = 0.2\boldsymbol{I}, \boldsymbol{\lambda}_2 = 0.01\boldsymbol{I}$
STSMC	$\boldsymbol{\alpha}_1 = 0.05\boldsymbol{I}, \boldsymbol{\alpha}_2 = 0.2\boldsymbol{I}, \boldsymbol{\alpha}_3 = 0.1\boldsymbol{I}$
SSTESO	$\boldsymbol{\lambda}_1 = 0.4\boldsymbol{I}, \boldsymbol{\lambda}_2 = 0.2\boldsymbol{I}, \boldsymbol{\beta} = 100\boldsymbol{I}$
SSTSMC	$\boldsymbol{\alpha}_1 = 0.05\boldsymbol{I}, \boldsymbol{\alpha}_2 = 0.1\boldsymbol{I}, \boldsymbol{\alpha}_3 = 0.2\boldsymbol{I}, \boldsymbol{\beta} = 200\boldsymbol{I}$

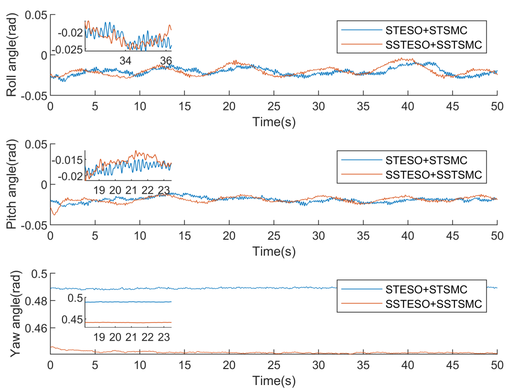

Fig. 3. Experimental curves of attitude angle in Simulation II

Fig. 3 and Fig. 4 show the attitude control and angular rate control performance on three channels with traditional super-twisting methods and sigmoid super-twisting methods, respectively. From Fig. 3, it can be seen that both methods can make reasonable adjustments to the stable attitude in order to resist the disturbance, but the proposed methods have better performance. In particular, the pitch angle is supposed to be 0 rad when quadrotor hovering, but the pitch curve is moving around -0.02 rad because of the additional disturbance. It can be also seen that in the Fig. 4, the chattering effect is smaller using sigmoid super-twisting methods, especially on roll channel. Although both methods can perform well under disturbance, the proposed SSTESO+SSTSMC method has less chattering effect than STESO+STSMC method. It can be verified that the introduction of sigmoid function not only can maintain the advantages of original super- twisting methods, but also reduce the chattering effect.

VI. CONCLUSIONS AND FUTURE WORK

In order to reduce the chattering effect of the original STESO and STSMC, we introduce a continuous sigmoid function for replacing the non-continuous signum function used in STESO and STSMC and propose SSTESO and SSTSMC. For further verification of our idea, we analyze

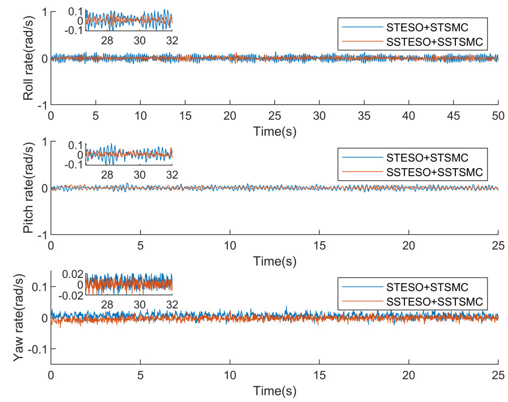

Fig. 4. Experimental curves of angular rate in Simulation II

the convergence using Lyapunov function and derive that the estimation error or attitude tracking error can converge to a bounded ball as time goes to infinity if the parameters chosen to satisfy the given convergence conditions. Besides, two simulations are performed in PX4/Gazebo environment for comparing the estimation and attitude control performance between original super-twisting methods and sigmoid super-twisting methods. The results show that the proposed methods not only keep the advantage of original super-twisting methods, but also have less chattering effect. In the future, we will implement our methods on the real quadrotor for further verification of our idea.

ACKNOWLEDGMENT

This work was supported by the National Key R&D Program of China (Grant No. 2017YFB1302503) and the National Natural Science Foundation of China (Grant No. 61633002)

REFERENCES

[1] K. Zhao, J. Zhang, D. Ma, and Y. Xia, "Composite disturbance rejection attitude control for quadrotor with unknown disturbance," *IEEE Transactions on Industrial Electronics*, 2019.

[2] M. J. Stepaniak, F. V. Graas, and M. U. De Haag, "Design of an electric propulsion system for a quadrotor unmanned aerial vehicle," *Journal of Aircraft*, vol. 46, no. 3, pp. 1050–1058, 2009.

[3] R. Ding, R. Jiao, and W. Chou, "Adaptive robust control for quad-rotor based on a compound control method," in *2017 36th Chinese Control Conference (CCC)*. IEEE, 2017, pp. 4887–4893.

[4] F. Kendoul, "Survey of advances in guidance, navigation, and control of unmanned rotorcraft systems," *Journal of Field Robotics*, vol. 29, no. 2, pp. 315–378, 2012.

[5] S. Gupte, P. I. T. Mohandas, and J. M. Conrad, "A survey of quadrotor unmanned aerial vehicles," in *2012 Proceedings of IEEE Southeastcon*. IEEE, 2012, pp. 1–6.

[6] M. A. Lotufo, L. Colangelo, C. Perez-Montenegro, E. Canuto, and C. Novara, "Uav quadrotor attitude control: An adrc-emc combined approach," *Control Engineering Practice*, vol. 84, pp. 13–22, 2019.

[7] L. Zhao, L. Dai, Y. Xia, and P. Li, "Attitude control for quadrotors subjected to wind disturbances via active disturbance rejection control and integral sliding mode control," *Mechanical Systems and Signal Processing*, vol. 129, pp. 531–545, 2019.

[8] A. L. Salih, M. Moghavvemi, H. A. Mohamed, and K. S. Gaeid, "Flight pid controller design for a uav quadrotor," *Scientific research and essays*, vol. 5, no. 23, pp. 3660–3667, 2010.

[9] X. Wu, B. Xiao, and Y. Qu, "Modeling and sliding mode-based attitude tracking control of a quadrotor uav with time-varying mass," *ISA transactions*, 2019.

[10] T. Madani and A. Benallegue, "Backstepping control for a quadrotor helicopter," in *2006 IEEE/RSJ International Conference on Intelligent Robots and Systems*. IEEE, 2006, pp. 3255–3260.

[11] C. Nicol, C. Macnab, and A. Ramirez-Serrano, "Robust adaptive control of a quadrotor helicopter," *Mechatronics*, vol. 21, no. 6, pp. 927–938, 2011.

[12] R. Xu and U. Ozguner, "Sliding mode control of a quadrotor helicopter," in *Proceedings of the 45th IEEE Conference on Decision and Control*. IEEE, 2006, pp. 4957–4962.

[13] A. Aboudonia, A. El-Badawy, and R. Rashad, "Active anti-disturbance control of a quadrotor unmanned aerial vehicle using the command-filtering backstepping approach," *Nonlinear Dynamics*, vol. 90, no. 1, pp. 581–597, 2017.

[14] S. Li, J. Yang, W.-H. Chen, and X. Chen, *Disturbance observer-based control: methods and applications*. CRC press, 2016.

[15] Y. Guo, B. Jiang, and Y. Zhang, "A novel robust attitude control for quadrotor aircraft subject to actuator faults and wind gusts," *IEEE/CAA Journal of Automatica Sinica*, vol. PP, no. 1, pp. 1–9, 2018.

[16] A. A. Godbole, J. P. Kolhe, and S. E. Talole, "Performance analysis of generalized extended state observer in tackling sinusoidal disturbances," *IEEE Transactions on Control Systems Technology*, vol. 21, no. 6, pp. 2212–2223, 2012.

[17] D. Shi, Z. Wu, and W. Chou, "Super-twisting extended state observer and sliding mode controller for quadrotor uav attitude system in presence of wind gust and actuator faults," *Electronics*, vol. 7, no. 8, p. 128, 2018.

[18] G. Gandikota and D. K. Das, "Disturbance observer–based adaptive boundary layer sliding mode controller for a type of nonlinear multiple-input multiple-output system," *International Journal of Robust and Nonlinear Control*, 2019.

[19] P. V. Suryawanshi, P. D. Shendge, and S. B. Phadke, "A boundary layer sliding mode control design for chatter reduction using uncertainty and disturbance estimator," *International Journal of Dynamics and Control*, vol. 4, no. 4, pp. 456–465, 2016.

[20] B. Tian, L. Liu, H. Lu, Z. Zuo, Q. Zong, and Y. Zhang, "Multivariable finite time attitude control for quadrotor uav: Theory and experimentation," *IEEE Transactions on Industrial Electronics*, vol. 65, no. 3, pp. 2567–2577, 2017.

[21] X. Shao and H. Wang, "Back-stepping robust trajectory linearization control for hypersonic reentry vehicle via novel tracking differentiator," *Journal of the Franklin Institute*, vol. 353, no. 9, pp. 1957–1984, 2016.

[22] L. R. G. Carrillo, A. E. D. López, R. Lozano, and C. Pégard, *Quad rotorcraft control: vision-based hovering and navigation*. Springer Science & Business Media, 2012.

[23] L. Meier, D. Honegger, and M. Pollefeys, "Px4: A node-based multithreaded open source robotics framework for deeply embedded platforms," in *2015 IEEE international conference on robotics and automation (ICRA)*. IEEE, 2015, pp. 6235–6240.

[24] L. Meier, P. Tanskanen, L. Heng, G. H. Lee, F. Fraundorfer, and M. Pollefeys, "Pixhawk: A micro aerial vehicle design for autonomous flight using onboard computer vision," *Autonomous Robots*, vol. 33, no. 1-2, pp. 21–39, 2012.

Appendix

The derivative of Lyapunov function of the proposed Lyapunov function V can be written as

$$\dot{V} = (\lambda_1^2 + 4\lambda_2)\mu_1\dot{\mu}_1 - \lambda_1\dot{\mu}_1\mu_2 - \lambda_1\mu_1\dot{\mu}_2 + 2\mu_2\dot{\mu}_2 \quad \text{(A1-1)}$$

From the first part of (A1-1), we can get

$$\begin{aligned}(\lambda_1^2 + 4\lambda_2)\mu_1\dot{\mu}_1 &= (\lambda_1^2 + 4\lambda_2)|z_1|^{\frac{1}{2}}\mathrm{sgn}(z_1)(-\frac{\lambda_1}{2}\mathrm{sgn}(z_1) \\ &\quad + \frac{1}{2}|z_1|^{-\frac{1}{2}}z_2) \\ &= (\lambda_1^2 + 4\lambda_2)(-\frac{\lambda_1}{2}|z_1|^{\frac{1}{2}} + \frac{1}{2}\mathrm{sgn}(z_1)z_2)\end{aligned} \quad \text{(A1-2)}$$

The second part of (A1-1) can be written as

$$-\lambda_1\dot{\mu}_1\mu_2 = \frac{\lambda_1^2}{2}\mathrm{sgn}(z_1)z_2 - \frac{\lambda_1}{2}|z_1|^{-\frac{1}{2}}z_2^2 \quad \text{(A1-3)}$$

The third part of (A1-1) yields

$$\begin{aligned}-\lambda_1\mu_1\dot{\mu}_2 &= -\lambda_1|z_1|^{\frac{1}{2}}\mathrm{sgn}(z_1)(-\lambda_2 sig(z_1) + \varepsilon) \\ &= \lambda_1\lambda_2|z_1|^{\frac{1}{2}} sig(z_1)\mathrm{sgn}(z_1) - \lambda_1|z_1|^{\frac{1}{2}}\varepsilon\mathrm{sgn}(z_1) \\ &\le \lambda_1\lambda_2|z_1|^{\frac{1}{2}} - \lambda_1|z_1|^{\frac{1}{2}}\varepsilon\mathrm{sgn}(z_1)\end{aligned} \quad \text{(A1-4)}$$

The fourth part of (A1-1) can be rewritten as

$$2\mu_2\dot{\mu}_2 = -2\lambda_2 sig(z_1)z_2 + 2z_2\varepsilon \quad \text{(A1-5)}$$

For further derivation, the following equations are given

$$\begin{aligned}\left|\mathrm{sgn}(z_1) - \frac{1 - e^{-\beta z_1}}{1 + e^{-\beta z_1}}\right| &= \left|\frac{2}{1 + e^{\beta|z_1|}}\right| \\ &\le \frac{2}{1 + \beta\,|z_1|} \le \frac{1}{\sqrt{\beta}|z_1|^{\frac{1}{2}}}\end{aligned} \quad \text{(A1-6)}$$

$$|z_2| \le \frac{1}{4} + z_2^2 \quad \text{(A1-7)}$$

$$2\,|\mu_2|\,|\mu_1| \le \mu_1^2 + \mu_2^2 \quad \text{(A1-8)}$$

According to (A1-1)-(A1-8), we can derive

$$\begin{aligned}\dot{V} &\le -(\tfrac{\lambda_1^3}{2} + \lambda_1\lambda_2)|z_1|^{\frac{1}{2}} + \lambda_1^2\mathrm{sgn}(z_1)z_2 + 2\lambda_2(\mathrm{sgn}(z_1) \\ &\quad - sig(z_1))z_2 - \tfrac{\lambda_1}{2}|z_1|^{-\frac{1}{2}}z_2^2 - \lambda_1|z_1|^{\frac{1}{2}}\varepsilon\mathrm{sgn}(z_1) + 2z_2\varepsilon \\ &\le -\left(\tfrac{\lambda_1^3}{2} + \lambda_1\lambda_2\right)|z_1|^{\frac{1}{2}} + \lambda_1^2\mathrm{sgn}(z_1)z_2 + \tfrac{2\lambda_2}{\sqrt{\beta}}|z_1|^{-\frac{1}{2}}\,|z_2| \\ &\quad - \tfrac{\lambda_1}{2}|z_1|^{-\frac{1}{2}}z_2^2 - \lambda_1|z_1|^{\frac{1}{2}}\varepsilon\mathrm{sgn}(z_1) + 2z_2\varepsilon \\ &\le -\tfrac{\lambda_1}{2}|z_1|^{-\frac{1}{2}}[(\lambda_1^2 + 2\lambda_2)\,|z_1| - 2\lambda_1|z_1|^{\frac{1}{2}}\mathrm{sgn}(z_1)z_2 + (1 - \tfrac{4\lambda_2}{\lambda_1\sqrt{\beta}})z_2^2 \\ &\quad - \tfrac{\lambda_2}{\lambda_1\sqrt{\beta}}] + \tfrac{\lambda_1}{2}|z_1|^{-\frac{1}{2}}(-2\,|z_1|\,\mathrm{sgn}(z_1) + \tfrac{4}{\lambda_1}|z_1|^{\frac{1}{2}}z_2)\varepsilon \\ &\le -\tfrac{\lambda_1}{2}|z_1|^{-\frac{1}{2}}[(\lambda_1^2 + 2\lambda_2)\mu_1^2 - 2\lambda_1\mu_1\mu_2 + (1 - \tfrac{4\lambda_2}{\lambda_1\sqrt{\beta}})\mu_2^2 \\ &\quad - \tfrac{\lambda_2}{\lambda_1\sqrt{\beta}}] + \tfrac{\lambda_1}{2}|z_1|^{-\frac{1}{2}}(2\mu_1^2 + \tfrac{4}{\lambda_1}\,|\mu_1|\,|\mu_2|)\varepsilon \\ &\le -\tfrac{\lambda_1}{2}|z_1|^{-\frac{1}{2}}[(\lambda_1^2 + 2\lambda_2)\mu_1^2 - 2\lambda_1\mu_1\mu_2 + (1 - \tfrac{4\lambda_2}{\lambda_1\sqrt{\beta}})\mu_2^2 \\ &\quad - \tfrac{\lambda_2}{\lambda_1\sqrt{\beta}}] + \tfrac{\lambda_1}{2}|z_1|^{-\frac{1}{2}}(2\mu_1^2 + \tfrac{2}{\lambda_1}|\mu_1|^2 + \tfrac{2}{\lambda_1}|\mu_2|^2)\varepsilon\end{aligned} \quad \text{(A1-9)}$$